Supplementary Material to the article "Bright Compton source based on the interaction of an ultraintense laser pulse with a relativistically transparent foil and a plasma mirror"

References to equations and figures without the letter S refer to the main text of the article. The notation is the same: $n_0 = N_e/N_c$ is the electron density of the foil normalized to the critical density, l is the foil thickness, $l^* = a_0\lambda/(\sqrt{2}\,\pi n_0)$ is the transparency threshold (1), $a_0 = 26.7$, and $\lambda = 800$ nm.

S1. Analysis of electron trajectories

To verify the mechanism of electron injection into the region of the field maximum, the trajectories of the foil electrons were recorded in simulations with plasma parameters close to the optimal ones ($n_0 = 45$–55, $l = (0.06$–$0.075)\lambda$), see Fig. S1. By the time the pulse reaches the mirror ($t = 78$ fs), the electrons with energies above 25 MeV form two groups (Fig. S1a). The first group is located at the leading edge of the transmitted pulse: these electrons left the foil at the moment it became transparent, 6–11 fs before the arrival of the field maximum, and their energy does not exceed 45 MeV. The second group consists of the bunches ejected from the foil while the most intense part of the pulse passes through it; these bunches are located near the pulse maximum. All electrons with energies above 45 MeV belong to this group. For comparison, Fig. S1a shows test electrons from a simulation in which the electron density of the foil was negligibly small and collective fields were absent: all of them are gathered at the leading edge of the pulse, and their energy does not exceed 25 MeV.

The energy of the bunch electrons varies non-monotonically (Fig. S1b): it follows the transverse momentum as the electron slips in phase with respect to the wave. Splitting the energy gain into the work done by the transverse field of the wave and the work done by the longitudinal field (Fig. S1c) shows that after leaving the foil the bunch electrons gain energy only from the wave field (about 50 MeV on average). The longitudinal charge-separation field decelerates them and takes away about 20 MeV on average, which does not change the qualitative picture. For the leading-edge electrons, the work of this field is negligible. Thus, the role of the foil is to inject electrons into the region of the field maximum, where they are accelerated directly by the field of the transmitted wave.

S2. Electron spectra

The spectra of the electrons moving in the direction of pulse propagation are shown in Fig. S2. They are nonthermal but broad and show no formation of quasi-monoenergetic bunches. The spectra have a pronounced cutoff energy, which reaches its maximum at the same parameters as the number of high-energy electrons (Fig. 3 of the main text). At $n_0 = 55$ (Fig. S2a), the spectrum extends up to ≈ 95 MeV only in a narrow interval of thicknesses $l = (0.05$–$0.067)\lambda$, i.e., at $l = (0.46$–$0.61)\,l^*$. Already at $l = 0.071\lambda$, the cutoff energy drops to 55–70 MeV, and then it slowly decreases as the thickness increases. At $l = 0.06\lambda$ (Fig. S2b), the cutoff energy grows with n_0 from ≈ 35 MeV at $n_0 = 15$ to 90–96 MeV at $n_0 = 45$ and 55, and with a further increase in n_0 it decreases again to 65–70 MeV. As in the maps of Fig. 3 of the main text, this dependence is non-monotonic: at $n_0 = 50$, the cutoff is only ≈ 70 MeV. Thus, the optimum corresponds to the most efficient injection of electrons into the region of the field maximum. The hard part of the photon spectrum (Figs. 4d and 4e of the main text) follows the cutoff energy of the electrons.

S3. Collision stage

Figure S3 shows the collision of the accelerated electrons with the pulse reflected from the mirror at $n_0 = 55$, $l = 0.06\lambda$, and $t = 81$ fs. Part of the electrons located at the front of the transmitted pulse fly further without taking part in the collision with the reflected radiation. Therefore, only about 80 % of the electrons with energies above 25 MeV are involved in inverse Compton scattering.

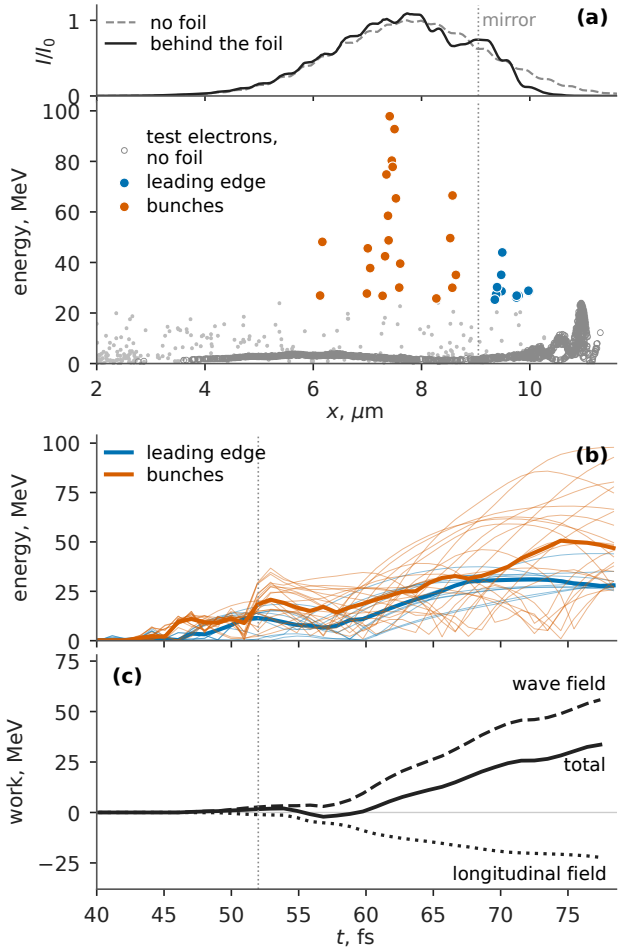


Fig. S1. Trajectories of the foil electrons in simulations with $n_0 = 45$–55, $l = (0.06$–$0.075)\lambda$. (a) Time $t = 78$ fs: period-averaged on-axis intensity behind the foil and without the foil (top) and energy of the tracked electrons versus coordinate (bottom). Electrons with energies above 25 MeV at the leading edge of the pulse and in the bunches are highlighted in color, circles show test electrons in the simulation without collective fields. (b) Energy of the highlighted electrons versus time, thick lines are the medians over the groups. (c) Work done by the transverse field of the wave and by the longitudinal field after leaving the foil, averaged over the bunch electrons. The vertical dotted line in (b) and (c) marks the arrival of the pulse maximum at the foil.

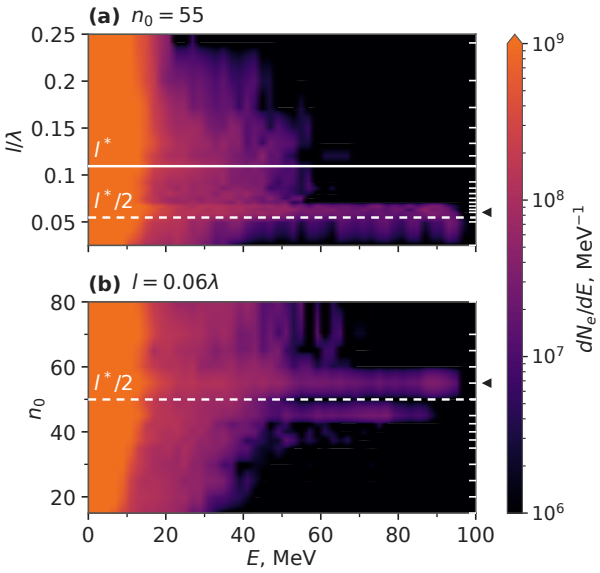


Fig. S2. Spectra of the electrons moving in the direction of pulse propagation at $t = 75$ fs: (a) versus the foil thickness at $n_0 = 55$; (b) versus n_0 at $l = 0.06\lambda$ (linear interpolation between the simulations, whose positions are marked by ticks on the right; the size along the third coordinate is taken equal to 5 μm). The solid line is $l = l^*$, the dashed lines are $l = l^*/2$, and the triangles mark the values $l = 0.06\lambda$ and $n_0 = 55$.

This can be seen from a comparison of the phase portraits of electrons and photons (Figs. S3b and S3c): photons with energies above 100 keV are not emitted by the leading-edge electrons and appear only for the electrons that follow behind them. The maxima of the photon momentum coincide with the maxima of the electron momentum, i.e., the hardest photons are emitted by the most energetic electrons. The photons of the second emission stage are emitted near the mirror surface (Fig. S3a). Their characteristics are shown in Fig. 4 of the main text.

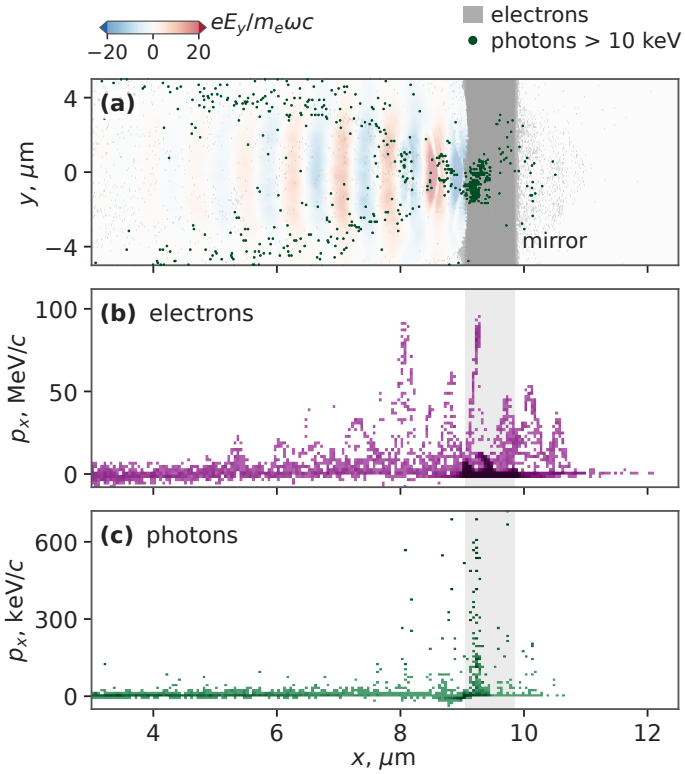


Fig. S3. Collision stage at $n_0 = 55$, $l = 0.06\lambda$, and $t = 81$ fs. (a) Field E_y (color scale), electrons (gray), and photons with energies above 10 keV (green dots); the mirror is the gray band at $x = 9$–10 μm. (b) x–p_x phase portrait of the electrons. (c) The same for the photons. The light gray band marks the position of the mirror.

S4. Angular distribution and solid angle of the emission

The energy distribution of the electrons over p_y/p (Fig. 4c of the main text) has two maxima at $|p_y/p| \approx 0.2$–0.27 ($\vartheta \approx 12°$–$16°$). They are due to the transverse momentum of the electrons in the field of the linearly polarized wave (its projection is seen in the simulation plane). Hard photons with $p_x c > 100$ keV reproduce this two-lobe structure: the maxima of their distribution (Fig. 4f of the main text) are located at $|p_y/p| \approx 0.13$–0.17 ($\vartheta \approx 8°$–$10°$), and 80 % of the energy is emitted within $|p_y/p| < 0.25$. The distribution of softer photons with $p_x c = 10$–100 keV is much broader: it is almost uniform up to $|p_y/p| \approx 0.7$ ($\vartheta \approx 45°$) and has a dip near the axis. This is a consequence of the wiggler regime of scattering with the parameter $K = a \gg 1$: the radiation from different parts of the trajectory is emitted at different angles within K/γ in the polarization plane [1]. In projection onto the simulation plane at $K = a_0$, this angle ranges from 5° at $\gamma = 200$ to 27° at $\gamma = 40$. The hardest photons are emitted by the most energetic electrons, for which this angle is small, while the soft part of the spectrum is formed by electrons with lower energies.

When the solid angle $\Delta\Omega$ of the emission is estimated, it must be taken into account that the emission is not axially symmetric. The electrons oscillate in the polarization plane, which makes an angle of 45° with the simulation plane, and the photons are emitted into a fan elongated along this plane. The distributions in Fig. 4f of the main text are the projection of this fan onto the simulation plane. This is also indicated by the sharp cutoff of the distribution of 10–100 keV photons

at $|p_y/p| \approx 0.77$, which is close to $1/\sqrt{2} \approx 0.71$ and would be absent for an axially symmetric emission. The thickness of the fan is determined by the spread of the electron momenta across the polarization plane. For the recorded trajectories of electrons with energies above 30 MeV, this spread is $\delta p_\perp \approx 7 m_e c$, while the spread along the polarization plane is $\approx 30 m_e c$.

If σ_y is the rms value of p_y/p for the photons of a given energy interval, then the angular half-width of the fan along the polarization plane is $\sigma_\parallel \approx (2\sigma_y^2 - \sigma_\perp^2)^{1/2}$, and the half-width across it is $\sigma_\perp \approx \delta p_\perp/(\gamma m_e c)$. For a Gaussian distribution, the region that contains 80 % of the energy has the solid angle $\Delta\Omega \approx 2\pi \ln 5\, \sigma_\parallel \sigma_\perp$. With $\sigma_y = 0.21$, $\sigma_\perp \approx 0.07$ for photons with energies above 100 keV and $\sigma_y = 0.5$, $\sigma_\perp \approx 0.2$ for 10–100 keV photons, this gives ≈ 0.2 and ≈ 1.4 sr, respectively. To refine these values, we used a test-particle model. In this model, electrons with momenta taken from the recorded trajectories collided with a counterpropagating plane wave of amplitude 20–35 with the polarization of the reflected pulse. The radiation was calculated from the local synchrotron spectrum and directed along the electron momentum. The model reproduces the position of the lobes of the hard-photon distribution ($|p_y/p| \approx 0.2$ versus 0.17 in the kinetic simulation). In the model, the ratio of the solid angle of the fan to the solid angle of the annular cone constructed from the same projection is 0.6–0.7 for soft photons and 0.4–0.5 for hard photons. Applying this ratio to the distributions obtained in the kinetic simulation, we find that 80 % of the energy of the second-stage radiation is contained within a solid angle of ≈ 1.2 sr (1.1–1.3 sr) for 10–100 keV photons and ≈ 0.13 sr (0.11–0.18 sr) for photons with energies above 100 keV. These values are used in the main text to estimate the brightness. For the radiation of all three stages, which is used in the comparison with the experiment [2], the same ratio gives ≈ 1 sr above 10 keV and ≈ 0.4 sr above 100 keV. This estimate is rougher, since the model was built for the second stage.

1. S. Corde, K. Ta Phuoc, G. Lambert, R. Fitour, V. Malka, A. Rousse, A. Beck, and E. Lefebvre, "Femtosecond x rays from laser-plasma accelerators", Rev. Mod. Phys. **85**, 1 (2013).

2. Y. Shou, P. Wang, S. G. Lee et al., "Brilliant femtosecond-laser-driven hard X-ray flashes from carbon nanotube plasma", Nat. Photonics **17**, 137 (2023).